Science and Technology Indonesia
e-ISSN:2580-4391 *p*-ISSN:2580-4405
Vol. 10, No. 2, April 2025

Research Paper

Ferulic Acid-Nicotinamide Cocrystal: Synthesis, Experimental, and Computation Study

Fery Eko Pujiono[1,2], Juni Ekowati[3], Tahta Amrillah[4], Dwi Setyawan[3]*

[1]*Department of Pharmacy, Faculty of Pharmacy, Institut Ilmu Kesehatan Bhakti Wiyata, Kediri, 64114, Indonesia*
[2]*Doctoral of Pharmacy, Faculty of Pharmacy, Universitas Airlangga, Surabaya, 60115, Indonesia*
[3]*Department of Pharmaceutical Sciences, Faculty of Pharmacy, Universitas Airlangga, Surabaya, 60115, Indonesia*
[4]*Department of Engineering, Faculty of Advanced Technology and Multidiscipline, Universitas Airlangga, Surabaya, 60115, Indonesia*
***Corresponding author**: dwisetyawan-90@ff.unair.ac.id

Abstract
Ferulic acid-nicotinamide cocrystals have been successfully synthesized using the solvent evaporation method. In this case, nicotinamide which acts as a coformer is mixed with ferulic acid with a 1:1 molar ratio via dissolving process in ethanol. The obtained cocrystals were characterized through Differential Scanning Calorimetric (DSC), Powder X-Ray Diffraction (PXRD), Fourier-transform infrared spectroscopy (FTIR), scanning electron microscopy (SEM), and computational analyses. The DSC characterization revealed distinct endothermic peaks at 99.5°C and 128.5°C with a *W*-shaped profile. This result is different from the thermal behavior of pure ferulic acid which indicates that the ferulic acid-nicotinamide cocrystal is successfully formed. This result is also supported by the PXRD result which reveals distinct peaks at 5.24°, 16.31°, and 34.69° belong to crystal deformation of ferulic acid cocrystal due to the coexistence of nicotinamide coformer. The FTIR data also further indicate the formation of cocrystals marked by the disappearance of the $-NH(\nu)$ functional group at 3400 cm^{-1} and the emergence of a fuse-like peak at around 1600 cm^{-1} corresponding to the $C{=}O(\nu)$ and $-NH(\delta)$ functional groups. SEM analysis also demonstrated morphological differences between the obtained cocrystal with pure ferulic acid crystals. The pure ferulic acid crystals exhibit a rectangular shape, whereas the cocrystals display a sword-like morphology. The phenomenon of cocrystal formation was also studied using computational studies through Density Functional Theory (DFT) and Quantum Theory of Atoms in Molecules (QTAIM) which confirmed that the cocrystals were stabilized through intermolecular hydrogen bonding.

Keywords
Cocrystal, Ferulic Acid, Solvent Evaporation, DFT, QTAIM

Received: 5 November 2024, Accepted: 24 January 2025
https://doi.org/10.26554/sti.2025.10.2.402-410

1. INTRODUCTION

Ferulic acid ($C_{10}H_{10}O_4$) is a naturally occurring phenolic compound predominantly found in plants. This compound belongs to the hydroxynamic acid group and exhibits several significant biological activities (Fazeli, 2021; Li et al., 2021; Pyrzynska, 2024). Ferulic acid is a derivative of cinnamic acid commonly seen in plant cell walls, particularly in conjugated forms with polysaccharides and proteins. Ferulic acid occurs naturally in various crops, particularly in grains, including wheat, rice, corn, and oats. This chemical includes fruits like oranges and apples and vegetables such as broccoli and tomatoes. The principal source of ferulic acid in the industry often derives from rice or maize husks, which are then extracted and purified for several uses (Chaudhary et al., 2019; Dragan et al., 2018; Fazeli, 2021).

Ferulic acid exhibits significant antioxidant properties attributed to its molecular configuration, which includes hydroxyl ($-OH$) and methoxyl ($O-CH_3$) groups on aromatic rings, alongside a conjugated double bonding system that facilitates the stabilization of free radicals through electron delocalization (Li et al., 2021; Pyrzynska, 2024). It can neutralize free radicals that may harm cells, DNA, and proteins, diminishing the risk of degenerative diseases such as cancer, cardiovascular conditions, and premature aging (Chaudhary et al., 2023; Neopane et al., 2023). Moreover, ferulic acid demonstrates anti-inflammatory (Song et al., 2023), antibacterial (Jin et al., 2023), and antidiabetic effects (Khatun et al., 2024), rendering it a compelling option for diverse applications, ranging from food to medicines. However, ferulic acid presents a significant issue due to its low solubility in water, measured at 0.06 mg/mL (Contardi et al., 2021; Vilas-Boas et al., 2020). The primary reason for the low solubility of ferulic acid in water is the predominance of the hydrophobic characteristics of its aromatic ring and conjugated double-bond system (Cantele et al., 2023; Wang et al., 2021b).

Despite the presence of hydrophilic groups like hydroxyl and carboxylate, their strength is insufficient to counterbalance the overall hydrophobic characteristics of the molecule, hence diminishing the interaction between ferulic acid and water (Wang et al., 2021a). This issue must be addressed to enhance the solubility of ferulic acid, hence improving its bioavailability, one method being the creation of cocrystals.

A cocrystal is a crystalline entity composed of two or more constituents interconnected by non-covalent interactions, such as hydrogen bonds, van der Waals forces, or electrostatic interactions (Akhtaruzzaman et al., 2023; Panzade et al., 2024; Tupe et al., 2023). One component is the Active Pharmaceutical Ingredient (API) molecule, and the other is the coformer, a neutral molecule that enhances the physicochemical features of the API (Khan et al., 2023; Sulistyowaty et al., 2024; Wong et al., 2024). Conversely, ferulic acid possesses hydroxyl and carboxylate groups, which confer a notable advantage in cocrystal formation due to their capacity to establish robust hydrogen bonds, adaptability in engaging with diverse co-formers, and their influence on diminishing lattice energy (Wang et al., 2021a). The benefit of cocrystals is that they do not alter the structure of the primary molecules but instead reorganize the interactions among molecules in the solid state, thereby altering the related physical properties, including solubility and dissolution rate (Khan et al., 2023; Panzade et al., 2024; Tupe et al., 2023). These cocrystals enhance ferulic acid's solubility, thermal stability, chemical stability, and pharmacological efficacy (Liu et al., 2022; Xia et al., 2023). Cocrystal provides a more secure option than other methods, such as surfactants or organic solvents, which may exhibit adverse consequences (Nyamba et al., 2024; Panzade et al., 2024).

Aitipamula and Das (2020) synthesized ferulic acid cocrystals with isonicotinamide through the rotovap technique. Conversely, Yu et al. (2021) research demonstrated that ferulic acid and 5-fluorouracil cocrystal utilized the solvent evaporation technique. Liu et al. (2023) similarly researched the synthesis of theophylline and ferulic acid cocrystals using solvent evaporation. The research emphasizes the production and characterization of cocrystals; nevertheless, computational methods have not investigated intermolecular interactions. The research uniqueness is in the synthesis and characterization of cocrystals and the execution of computational intermolecular studies.

In this present study, the synthesis of ferulic acid cocrystals with nicotinamide conformers is conducted. The obtained sample then is characterized using Differential Scanning Calorimetric (DSC), Powder X-Ray Diffraction (PXRD), Fourier Transform Infrared (FTIR), and Scanning Electron Microscopy (SEM). Density Functional Theory (DFT) computations also have been conducted to ascertain intermolecular bonding and reactivity descriptors through Electrostatic Potential Surface (EPS) and Frontier Molecular Orbital (FMO) analyses. Furthermore, we examined the chemical bonding in cocrystal molecules utilizing Bader's Quantum Theory of Atoms in Molecules (QTAIM).

2. EXPERIMENTAL SECTION

2.1 Materials

The materials utilized in this study included trans-ferulic acid (HOC_6H_3 (OCH_3) $CH{=}CHCO_2H$, purity ≥99%, Sigma-Aldrich, Singapore), nicotinamide ($C_6H_6N_2O$, purity ≥98%, Sigma-Aldrich, Singapore), and ethanol (C_2H_5OH, purity ≥99.9%, Merck Millipore, Germany) as the solvent.

2.2 Methods

2.2.1 Preparation of Ferulic Acid-Nicotinamide Cocrystal by Solvent Evaporation

The synthesis of cocrystal is an adaptation of the research conducted by Yadav et al. (2024). In this method, 1.7 mg of ferulic acid and 0.3 mg of nicotinamide are dissolved in 10 mL of ethanol in a 1:1 molar ratio. The resulting mixture is stirred using a magnetic stirrer for 2 hours and subsequently evaporated at room temperature for 5 days until the cocrystal has dried. Cocrystals develop following a 5-day storage period in a desiccator.

2.2.2 Characterization

The cocrystal samples were characterized in the eutectic phase utilizing Differential Scanning Calorimetric (DSC) from Mettler Toledo over a temperature range of 30°C to 300°C, with a heating rate of 10°C/min. The crystal phase was measured using Powder X-Ray Diffraction (PXRD) from PANalytical X'Pert PRO at 2θ of 5.0084° to 59.98614°, with a step time of 10.1500 seconds and a step size of 0.0170°. The functional group of the sample was characterized using the Fourier Transform Infrared (FTIR) spectroscopy from Shimadzu IR-Prestige-21, equipped with a horizontal Golden-Gate MKII single reflection and wavelength range of 400 to 4000 cm^{-1}. Surface morphology was characterized using Scanning Electron Microscopy (SEM) from Hitachi Flexsem 100 with magnifications ranging from 500 to 5000×, with an applied voltage of 20.0 *kV*.

2.2.3 Computational Studies

The analysis of intermolecular interactions in cocrystals was conducted computationally using the Gaussian16 software, employing the Density Functional Theory (DFT) technique based on the Lee-Yang-Parr exchange-correlation functional (B3LYP) and the 6-311++G(d,p) basis set. Additionally, the outcomes of DFT were employed to ascertain topology and non-covalent interaction energies utilizing the Multiwfn 3.8 software, with visualization conducted through the Visual Molecular Dynamics (VMD) 1.9.4 application. Furthermore, the outcomes of DFT are employed for assessing chemical reactivity through the Electrostatic Potential Surface (EPS) and Frontier Molecular Orbital (FMO) methodologies.

3. RESULTS AND DISCUSSION

3.1 Analysis of Differential Scanning Calorimetry (DSC) Result

DSC is an instrument utilized to ascertain details regarding the eutectic phase, highlighting variations in eutectic peaks between BAF and cocrystal (Thayyil et al., 2020). Figure 1 displays the outcomes of the crystalline DSC analysis of ferulic acid, nicotinamide, and ferulic acid-nicotinamide cocrystal.

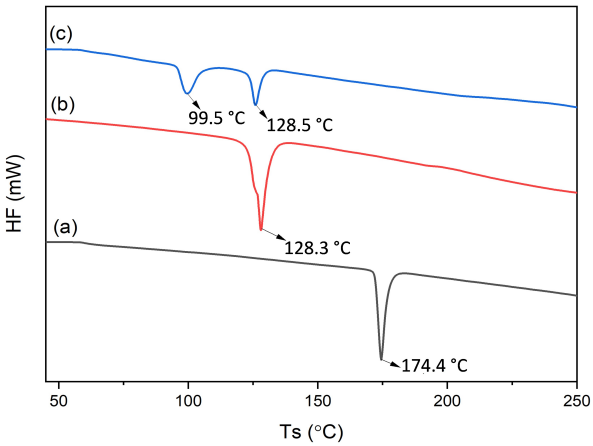

Figure 1. DSC Analysis Results: (a) Ferulic Acid, (b) Nicotinamide, and (c) Ferulic Acid-Nicotinamide Cocrystal

The DSC data in Figure 1 indicate that ferulic acid has an endothermic peak at 174.4°C, whereas nicotinamide displays an endothermic peak at 128.3°C. The cocrystal exhibited W-shaped endothermic maxima at 99.5°C and 128.5°C. Their melting point is inferior to that of any pure components, indicative of crystalline formation rather than a physical combination or simple salt (dos Santos et al., 2021; Thayyil et al., 2020).

3.2 Analysis of Powder X-Ray Diffraction (PXRD) Result

PXRD is an instrument utilised to confirm the development of cocrystal by generating a new diffractogram peak compared to the Active Pharmaceutical Ingredient (Hibbard et al., 2024). The analysis findings of the PXRD of ferulic acid, nicotinamide and ferulic acid-nicotinamide cocrystal are presented in Figure 2.

The diffractogram pattern is seen in Figure 2. dos Santos et al. (2021) demonstrated that ferulic acid exhibited distinct peaks at 2θ values of 8.98°, 10.45°, 12.78°, 15.60°, 17.37°, 26.43°, and 29.44°. Nicotinamide exhibits distinct peaks at 2θ: 14.75°, 22.17°, 23.30°, 25.33°, 25.79°, and 27.28°, as reported by Ding et al. (2023). The cocrystals have a distinct peak compared to the original molecules. The diffractogram pattern has distinct peaks at 2θ: 5.24°, 16.31°, and 34.69° corresponding to the cocrystal. The identified peaks signify that the cocrystal establishes a novel crystalline phase distinct from the original chemical (dos Santos et al., 2021; Hibbard et al., 2024).

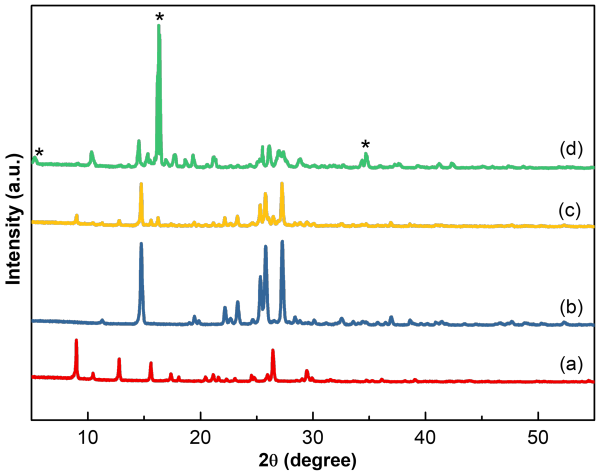

Figure 2. Results of PXRD Analysis: (a) Ferulic Acid; (b) Nicotinamide; (c) Ferulic Acid-Nicotinamide Physical Mixture; (d) Ferulic Acid-Nicotinamide Cocrystal

3.3 Analysis of Fourier Transform Infrared (FTIR) Spectroscopy Result

FTIR spectroscopy is a technique used to analyze hydrogen bonds by revealing the differences in infrared spectra between pure ferulic acid and its cocrystallized form, which is influenced by these bonds (Tatsumi et al., 2024). The FTIR analysis results of the ferulic acid, nicotinamide, ferulic acid-nicotinamide physical mixture, and ferulic acid-nicotinamide cocrystal are presented in Figure 3.

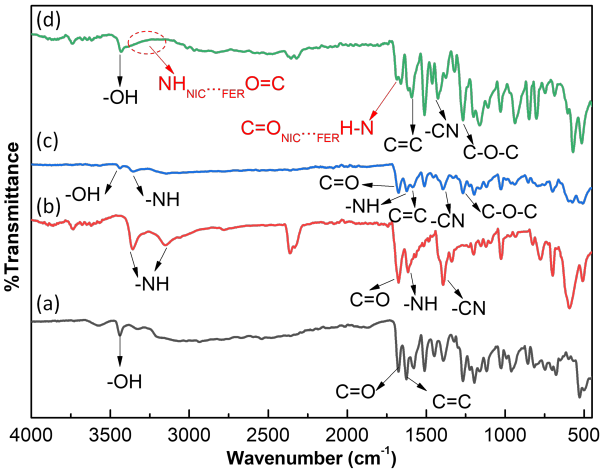

Figure 3. FTIR Analysis Results: (a) Ferulic Acid; (b) Nicotinamide; (c) Ferulic Acid-Nicotinamide Physical Mixture; (d) Ferulic Acid-Nicotinamide Cocrystal

The FTIR spectra depicted in Figure 3 reveal that ferulic acid exhibits distinct peaks at 3438 cm^{-1}, 1676 cm^{-1}, 1625 cm^{-1}, and 1264 cm^{-1}, corresponding to the functional groups −OH(ν), C=O(ν), C=C(ν), and C−O−C(ν), respectively, as

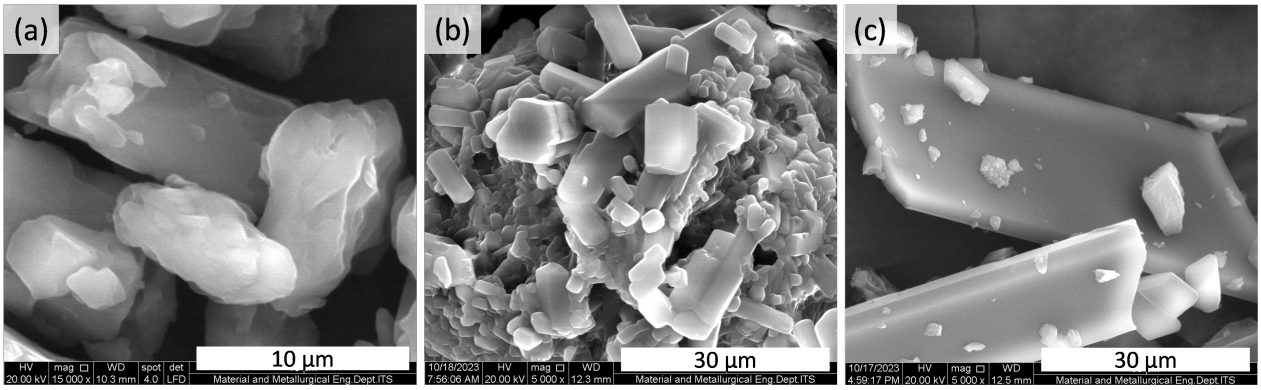

Figure 4. SEM analysis results: (a) Ferulic acid; (b) Nicotinamide; (c) Ferulic Acid-Nicotinamide Cocrystal

reported by dos Santos et al. (2021). Conversely, nicotinamide displays specific peaks at 3359 cm^{-1} and 3152 cm^{-1}, indicating the −NH(ν) functional group, while peaks at 1675 cm^{-1}, 1612 cm^{-1}, and 1391 cm^{-1} correspond to the C=O(ν), −NH(δ), and C−N(δ) functional groups, respectively, as demonstrated by Ding et al. (2023). The physical mixture exhibits no alteration, indicating the combination of ferulic acid and nicotinamide. The spectra of the cocrystals exhibited a distinction with the disappearance of the −NH(ν) functional group at approximately 3400 cm^{-1} and the emergence of a fuse-like peak at around 1600 cm^{-1}, precisely corresponding to the C=O(ν) and −NH(δ) functional groups. This outcome reveals that the creation of cocrystals is marked by the loss or alteration of absorption peaks, signifying the establishment of intermolecular hydrogen bonds (Hibbard et al., 2024; Tatsumi et al., 2024; Thayyil et al., 2020).

3.4 Analysis of Scanning Electron Microscopy (SEM) Result

Scanning Electron Microscopy (SEM) is employed to examine the morphology of the formed cocrystals (Karagianni et al., 2018). The morphological characteristics of the ferulic acid, nicotinamide, and ferulic acid-nicotinamide cocrystal are demonstrated in Figure 4(a)-(c), respectively.

The SEM results presented in Figure 4 reveal that the morphology of ferulic acid takes the form of a rectangle, consistent with the findings of dos Santos et al. (2021), while the morphology of nicotinamide is also rectangular, as observed by Ding et al. (2023). In contrast, the morphology of the cocrystal is sword-like, with this shape change occurring due to molecular interactions during the cocrystal formation process (Karagianni et al., 2018). This observation is further supported by the particle size distribution between the Active Pharmaceutical Ingredient (API) and the cocrystals, as depicted in Figure 5.

Figure 5 illustrates that the pore size distribution exhibits a disparity in pore size between the cocrystal and the Active Pharmaceutical Ingredient (API), implying that the cocrystal is synthesized from a combination of the API and the coformer. This outcome signifies the formation of the synthesized cocrystals.

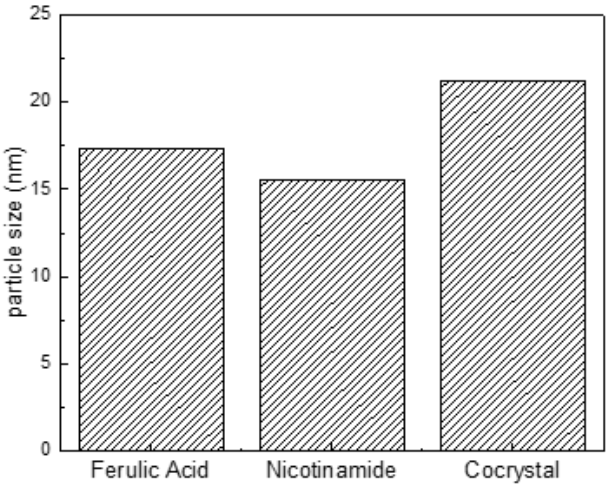

Figure 5. Distribution of Particle Size between Ferulic Acid, Nicotinamide, and Its Cocrystal

3.5 Analysis of Density Functional Theory (DFT) and Quantum Theory Atom in Molecules (QTAIM)

The characterization data indicate that cocrystal formation involves the establishment of intermolecular connections. This can be computationally predicted using Density Functional Theory (DFT) and Quantum Theory of Atoms in Molecules (QTAIM). DFT and QTAIM are computational methodologies that can elucidate intermolecular interactions, including their energy values (Birolo et al., 2024; Martín Pendás et al., 2023). This study employs DFT analysis utilizing the B3LYP/6-311G++ basis set (Hammami and Issaoui, 2022; Khan et al., 2023; Pujiono et al., 2024) Figure 6 displays the outcomes of the DFT study.

Figure 6 illustrates that cocrystals are generated by an intermolecular hydrogen bond between the C=O group of ferulic acid and the N−H group of nicotinamide, exhibiting a bond length of 1.206 Åand an interaction energy of -50.3255 kcal/mol. This signifies considerable stability from hydrogen bonding among molecular constituents (Huang et al., 2023).

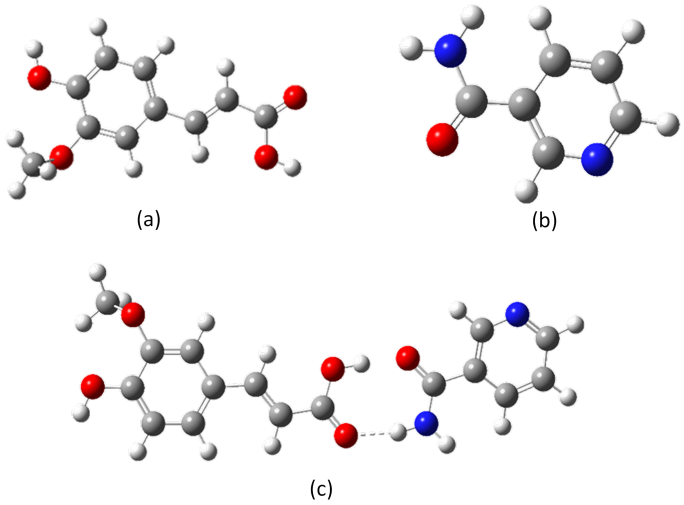

Figure 6. Geometric Optimization using DFT/B3LYP Calculations: (a) Ferulic Acid, (b) Nicotinamide, and (c) Ferulic Acid-Nicotinamide Cocrystal

Conversely, the formation of this cocrystallization does not influence the structure of ferulic acid, as evidenced by the bond length of C=O in individual ferulic acid measuring 1.226 Å, which changes to 1.225 Åupon cocrystallization, indicating that the cocrystal formation does not alter the structure of the Active Pharmaceutical Ingredient (API). According to the research conducted by Hammami and Issaoui (2022), intermolecular hydrogen bonds do not alter the length of API bonds by more than 1%. The findings of this DFT are corroborated by molecular geometry and isosurface results from Non-covalent Interaction (NCI) utilizing Multiwfn (Lu, 2024), as depicted in Figure 7.

The ferulic acid-nicotinamide cocrystal topology results with QTAIM in Figure 7(a) indicate that intermolecular hydrogen bonding between $C{=}O_{FER}\cdots_{NIC}NH$ and $OH_{FER}\cdots_{NIC}$ C=O facilitates the formation of cocrystals. This outcome is corroborated by an isosurface map, whereby hydrogen bonds are represented by blue chips and blue spikes at sign (λ_2) ρ equal to -0.04 a.u. This outcome is corroborated by the findings of the QTAIM through Bader topology, as presented in Table 1.

Table 1 indicates that the intermolecular bonds on $O_{13}\cdots H_{38}$ have an electron density of 0.0385 a.u. The Laplacian is 0.1196, whereas $H_{24}\cdots O_{32}$ has an electron density of 0.0567 a.u. with a Laplacian density of 0.1278. This is based on the research of Hammami and Issaoui (2022), which indicates that a positive value is a feature of intermolecular hydrogen bonding. This signifies a decrease in payload within the internuclear zone. Furthermore, the electron and Laplacian density values are ascertained using the Espinosa postulate, validating intermolecular hydrogen bonding (Espinosa et al., 1998; Hammami and Issaoui, 2022). Conversely, all topological parameters conform to the atomic interaction categorization derived from QTAIM analysis, specifically $\nabla 2\rho(r)>0$, $H(r)>0$, and $|V(r)|/G(r)<1$, indicating the presence of intermolecular hydrogen bonds with energies of -63.79 kJ/mol and -94.63 kJ/mol.

3.6 Analysis of Chemical Reactivity

Examining chemical reactivity in cocrystals seeks to ascertain the impact of molecular interactions on this reactivity (Khan et al., 2025). Chemical reactivity analyzed by DFT can be characterized by the Electrostatic Potential Surface (EPS) and Frontier Molecular Orbital (FMO) (Ali et al., 2024; Velmurugan et al., 2021).

EPS is a chemical reactivity analysis that reveals the findings of studies on the correlation between molecular structure and physicochemical attributes (Khan et al., 2025). The relationship is founded on the dipole moment, electronegativity, partial charge, and locus of chemical reactivity of a molecule. In EPS, variations in electrostatic potential are represented by distinct colors: red signifies negative electrostatic potential, blue denotes positive electrostatic potential, and green indicates zero electrostatic potential (Kanchana et al., 2023). The potential escalates with the color transition, specifically red<orange<yellow<green<blue (Kanchana et al., 2023; Singh et al., 2023). The EPS color code for ferulic acid ranges from -0.0892 a.u to 0.0892 a.u, but the ferulic acid-nicotinamide cocrystal range is -0.0836 a.u to 0.0836 a.u. The EPS mapping findings for ferulic acid and ferulic acid-nicotinamide cocrystal are presented in Figure 8.

Figure 8 illustrates that ferulic acid has a blue hue concentrated around the hydroxyl group, signifying a nucleophilic center and a red hue concentrated around the carboxylic group, indicating an electrophilic center. The development of cocrystals results in a color shift in the hydroxyl group of ferulic acid from blue to red or a reduction in electrostatic potential (Paneru et al., 2024). This suggests that the reduced electrostatic potential of the carboxyl group in ferulic acid results from the establishment of intermolecular hydrogen bonds, hence enhancing its reactivity (Aygün et al., 2024; Kanchana et al., 2023; Paneru et al., 2024). A reactivity analysis employed Frontier Molecular Orbital (FMO) theory to corroborate the EPS findings.

FMO is employed to forecast positional reactivity in conjugated systems. In the Frontier Orbital Analysis, the utilized metrics are the High Occupied Molecular Orbital (HOMO) and the Low Unoccupied Molecular Orbital (LUMO) (Kanchana et al., 2023; Singh et al., 2023). The HOMO and LUMO are critical factors in assessing the dynamic stability, chemical reactivity, and optical polarizability of high-energy materials (Singh et al., 2023). Figure 9 illustrates the findings of the HOMO and LUMO analyses for ferulic acid and ferulic acid-nicotinamide cocrystal.

Figure 9 indicates that the energy gap between HOMO and LUMO in the API and cocrystals is 0.2347 eV and 0.2229 eV, respectively. Reduced gap energies exhibit diminished stability and increased polarizability, resulting in heightened reactivity

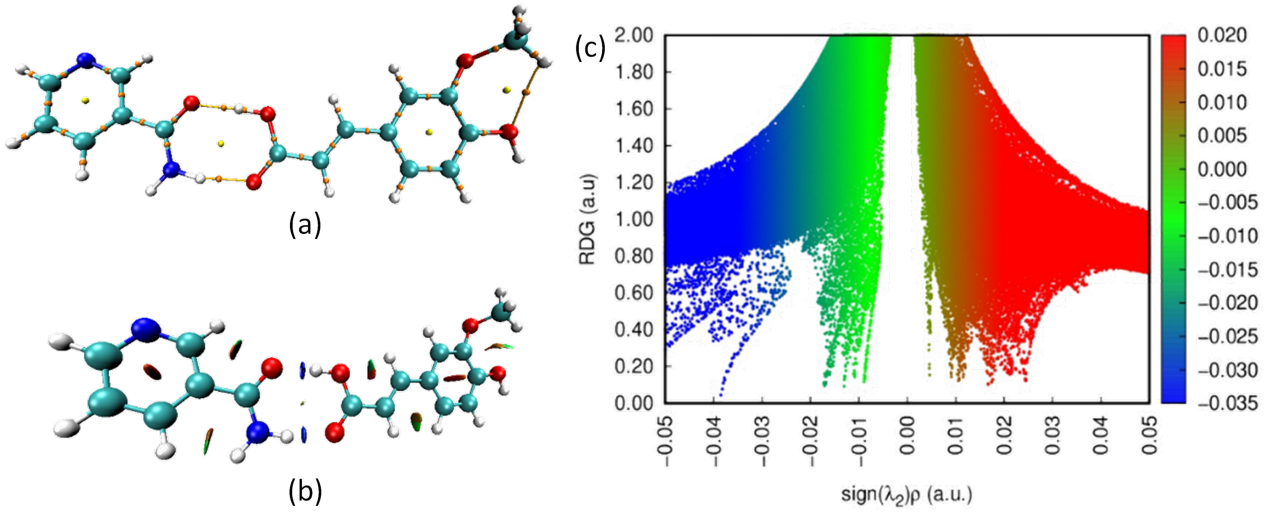

Figure 7. Results of NCI Analysis on Cocrystallization with QTAIM by Bader: (a) Molecular Geometry, (b) Isosurface Map, (c) Reduced Density Gradient (RDG) (Blue = Hydrogen Bond; Green = Van der Waals Bond; Red = Steric Effect)

Table 1. The Topological Parameters Obtained from the QTAIM Analysis

Material	+BCP	ρ (a.u)	$\nabla 2\rho$ (a.u)	G (a.u)	H (a.u.)	V (a.u)	$E_{H\cdots O}$ (kJ/mol)	ε (a.u)
Ferulic Acid-Nicotinamide Cocrystal	$O_{13}\cdots H_{38}$	0.0385	0.1196	0.0393	0.0094	-0.0486	-63.79	0.0053
	$H_{24}\cdots O_{32}$	0.0567	0.1278	0.0520	0.0200	-0.0721	-94.63	0.0022

+Bond critical point (BCP), electron density (ρ), Laplacian of electron density ($\nabla 2\rho$), Lagrangian kinetic energy (G), Hamiltonian kinetic energy (H), Potential energy density (V), Hydrogen bond Energy ($E_{H\cdots O}$), and eliplicity of electron density

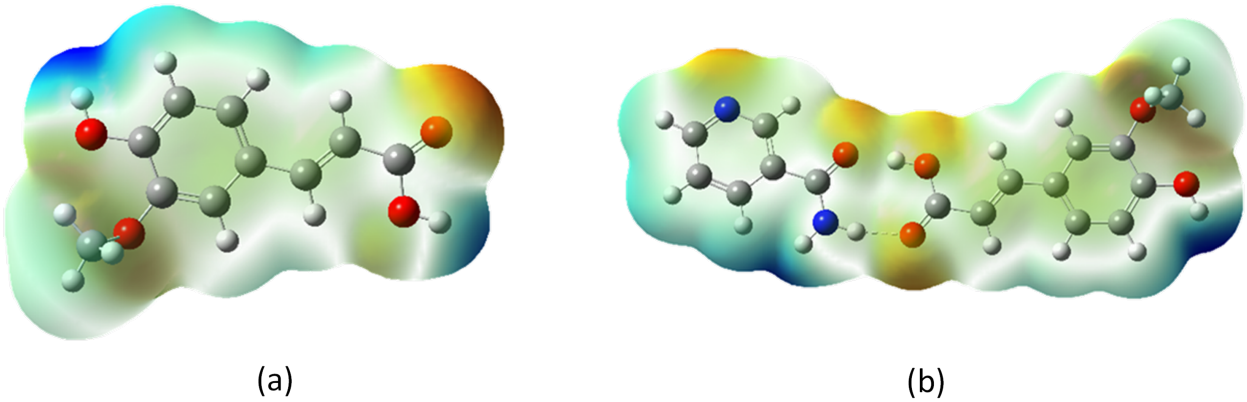

Figure 8. ESP Mapping on (a) Ferulic Acid and (b) Ferulic Acid-Nicotinamide Cocrystal

(Paneru et al., 2024; Szewczuk et al., 2023). This outcome is further corroborated by the Frontier Molecular Orbital (FMO) quantum chemistry descriptor presented in Table 2.

Table 2 indicates that the synthesized cocrystals exhibit reduced chemical hardness and enhanced chemical softness compared to the Active Pharmaceutical Ingredient (API). The results corroborate the HOMO-LUMO findings, wherein a significant S value suggests that the molecule is softer, indicating reduced stability and heightened reactivity. Hydrogen bonds in the cocrystals enhance their reactivity and facilitate interactions with solvents or other molecules, perhaps augmenting solubility (Miar et al., 2020; Paneru et al., 2024).

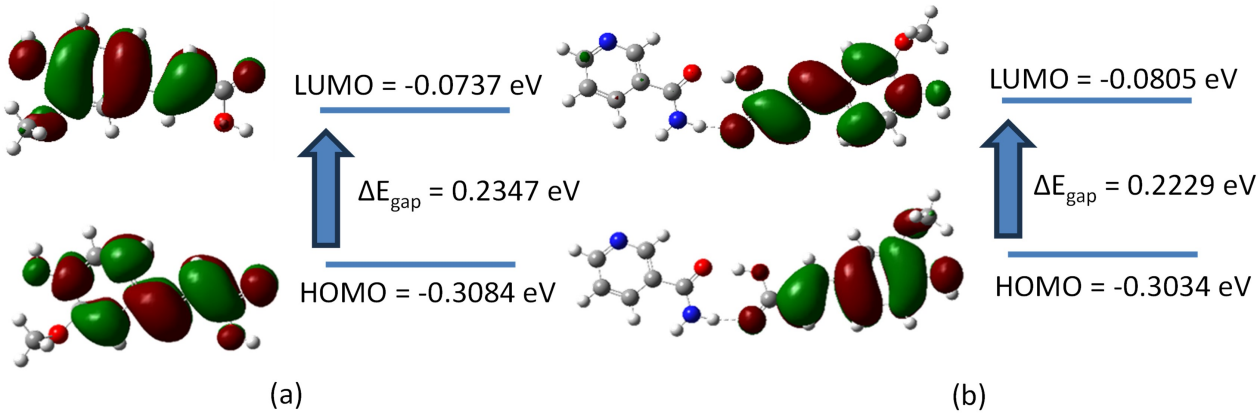

Figure 9. ESP Mapping on (a) Ferulic Acid and (b) Ferulic Acid-Nicotinamide Cocrystal

Table 2. Quantum Chemistry Descriptor from FMO

Materials	$+E_{LUMO}$ (eV)	E_{HOMO} (eV)	ΔE_{gap} (eV)	μ (eV)	η (eV)	S (eV)	χ (eV)	ω (eV)
FER	-0.0737	-0.3084	0.2347	-0.1910	0.1173	4.2607	0.1910	0.1555
Cocrystal	-0.0805	-0.3034	0.2229	-0.1919	0.1114	4.4863	0.1919	0.1653

+ Energy LUMO (E_{LUMO}), Energy HOMO (E_{HOMO}), Energy Gap (ΔE_{gap}), Chemical Potential (μ), Chemical Hardness (η), Softness (S), Electronegativity (χ) and Electrophilicity (ω)

4. CONCLUSIONS

The ferulic acid-nicotinamide cocrystals with 1:1 ratio is successfully fabricated using solvent evaporation method, as evidenced by characterization results of DSC, PXRD, FTIR, and SEM. The comprehensive characterization results indicate that the cocrystallization of ferulic acid with nicotinamide coformer has occurred through intermolecular linkages. This is corroborated by the findings from computations utilizing DFT and QTAIM. The QTAIM analysis results indicated that cocrystals formation were generated due to intermolecular hydrogen bonds between the C=O of ferulic acid and the N-H of nicotinamide coformers. This was further corroborated by QTAIM analysis, which demonstrated that cocrystals were formed through hydrogen intermolecular bonds between $C{=}O_{FER}\cdots_{NIC}NH$ and $OH_{FER}\cdots_{NIC}C{=}O$. The prediction of reactivity by DFT also indicated that hydrogen bonds in the cocrystals enhanced their reactivity and facilitated interactions with solvents or molecules.

5. ACKNOWLEDGMENT

The authors would like to express their gratitude to the Institut Ilmu Kesehatan Bhakti Wiyata and the Bhakti Wiyata Foundation for their financial support of this research.

REFERENCES

Aitipamula, S. and S. Das (2020). Cocrystal Formulations: A Case Study of Topical Formulations Consisting of Ferulic Acid Cocrystals. *European Journal of Pharmaceutics and Biopharmaceutics*, **149**; 95–104

Akhtaruzzaman, S. Khan, B. Dutta, T. S. Kannan, G. K. Kole, M. H. Mir, et al. (2023). Cocrystals for Photochemical Solid-State Reactions: An Account on Crystal Engineering Perspective. *Coordination Chemistry Reviews*, **483**; 215095

Ali, U. S., W. A. Siddiqui, A. Ashraf, M. A. Raza, K. M. Batoo, M. Imran, S. E. Shirsath, M. Ashfaq, M. N. Tahir, and S. Niaz (2024). Structure Elucidation {Single X-Ray Crystal Diffraction Studies, Hirshfeld Surface Analysis, DFT} and Antibacterial Studies of 1, 2-Benzothiazine Metal Complexes. *Journal of Molecular Structure*, **1306**; 137824

Aygün, M., D. B. Celepci, Ö. Akgül, and V. Pabuccuoglu (2024). Single-Crystal X-Ray Structure, Theoretical (Hirshfeld, Electronic Properties, NBO, NLO, RDG), and Molecular Docking Studies of Three Phthalimidoethanesulfonamide Derivatives. *Journal of Molecular Structure*; 139094

Birolo, R., E. Alladio, F. Bravetti, M. R. Chierotti, and R. Gobetto (2024). Predictive Tools for Cocrystal Formation. In *Novel Formulations and Future Trends*. Elsevier, pages 483–512

Cantele, C., K. Martina, G. Potenziani, A. M. Rossi, V. Cardenia, and M. Bertolino (2023). Antioxidant Properties of

Ferulic Acid-Based Lipophenols in Oil-In-Water (O/W) Emulsions. *LWT*, **189**; 115505

Chaudhary, A., V. S. Jaswal, S. Choudhary, A. Sharma, V. Beniwal, H. S. Tuli, and S. Sharma (2019). Ferulic Acid: A Promising Therapeutic Phytochemical and Recent Patents Advances. *Recent Patents on Inflammation & Allergy Drug Discovery*, **13**(2); 115–123

Chaudhary, P., P. Janmeda, A. O. Docea, B. Yeskaliyeva, A. F. Abdull Razis, B. Modu, D. Calina, and J. Sharifi-Rad (2023). Oxidative Stress, Free Radicals and Antioxidants: Potential Crosstalk in the Pathophysiology of Human Diseases. *Frontiers in Chemistry*, **11**

Contardi, M., M. Lenzuni, F. Fiorentini, M. Summa, R. Bertorelli, G. Suarato, and A. Athanassiou (2021). Hydroxycinnamic Acids and Derivatives Formulations for Skin Damages and Disorders: A Review. *Pharmaceutics*, **13**(7); 999

Ding, F., W. Cao, R. Wang, N. Wang, A. Li, Y. Wei, S. Qian, J. Zhang, Y. Gao, and Z. Pang (2023). Mechanistic Study on Transformation of Coamorphous Baicalein-Nicotinamide to Its Cocrystal Form. *Journal of Pharmaceutical Sciences*, **112**(2); 513–524

dos Santos, J. A. B., J. V. C. Júnior, R. S. de Araújo Batista, D. P. de Sousa, G. L. R. Ferreira, S. A. de Lima Neto, A. de Santana Oliveira, F. S. de Souza, and C. F. S. Aragão (2021). Preparation, Physicochemical Characterization and Solubility Evaluation of Pharmaceutical Cocrystals of Cinnamic Acid. *Journal of Thermal Analysis and Calorimetry*, **145**; 379–390

Dragan, M., C. D. Stan, A. T. Iacob, O. Dragostin, and L. Profire (2018). Ferulic Acid: Potential Therapeutic Applications. *The Medical-Surgical Journal*, **122**(2); 388–395

Espinosa, E., E. Molins, and C. Lecomte (1998). Hydrogen Bond Strengths Revealed by Topological Analyses of Experimentally Observed Electron Densities. *Chemical Physics Letters*, **285**(3–4); 170–173

Fazeli, F. (2021). Antioxidant Properties of Ferulic Acid on Cardiovascular Diseases. *International Journal of Advanced Biological and Biomedical Research*, **9**(3); 228–240

Hammami, F. and N. Issaoui (2022). A DFT Study of the Hydrogen Bonded Structures of Pyruvic Acid–Water Complexes. *Frontiers in Physics*, **10**; 901736

Hibbard, T., K. Shankland, and H. Al-Obaidi (2024). Preparation and Formulation of Progesterone Para-Aminobenzoic Acid Co-Crystals with Improved Dissolution and Stability. *European Journal of Pharmaceutics and Biopharmaceutics*, **196**; 114202

Huang, S., V. K. R. Cheemarla, D. Tiana, and S. E. Lawrence (2023). Experimental and Theoretical Investigation of Hydrogen-Bonding Interactions in Cocrystals of Sulfaguanidine. *Crystal Growth & Design*, **23**(4); 2306–2320

Jin, C., H. Zhang, F. Ren, J. Wang, and S. Yin (2023). Preparation and Characterization of Ferulic Acid Wheat Gluten Nanofiber Films with Excellent Antimicrobial Properties. *Foods*, **12**(14); 2778

Kanchana, S., T. Kaviya, P. Rajkumar, M. D. Kumar, N. Elangovan, and S. Sowrirajan (2023). Computational Investigation of Solvent Interaction (TD-DFT, MEP, HOMO-LUMO), Wavefunction Studies and Molecular Docking Studies of 3-(1-(3-(5-((1-Methylpiperidin-4-Yl)Methoxy)Pyrimidin-2-Yl)Benzyl)-6-Oxo-1,6-Dihydropyridazin-3-Yl)Benzonitrile. *Chemical Physics Impact*, **7**; 100263

Karagianni, A., M. Malamatari, and K. Kachrimanis (2018). Pharmaceutical Cocrystals: New Solid Phase Modification Approaches for the Formulation of APIs. *Pharmaceutics*, **10**(1); 18

Khan, A., N. Agrawal, R. Chaudhary, A. Yadav, J. Pandey, A. Narayan, S. Ali, P. Tandon, and V. R. Vangala (2025). Study of Chemical Reactivity and Molecular Interactions of the Hydrochlorothiazide-4-Aminobenzoic Acid Cocrystal Using Spectroscopic and Quantum Chemical Approaches. *Spectrochimica Acta Part A: Molecular and Biomolecular Spectroscopy*, **324**; 124960

Khan, I. M., A. Khan, S. Shakya, and M. Islam (2023). Exploring the Photocatalytic Activity of Synthesized Hydrogen Bonded Charge Transfer Co-Crystal of Chloranilic Acid with 2-Ethylimidazole: DFT, Molecular Docking and Spectrophotometric Studies in Different Solvents. *Journal of Molecular Structure*, **1277**; 134862

Khatun, M. M., M. S. Bhuia, R. Chowdhury, S. Sheikh, A. Ajmee, F. Mollah, M. S. Al Hasan, H. D. M. Coutinho, and M. T. Islam (2024). Potential Utilization of Ferulic Acid and Its Derivatives in the Management of Metabolic Diseases and Disorders: An Insight into Mechanisms. *Cellular Signalling*, **121**; 111291

Li, D., Y. Rui, S. Guo, F. Luan, R. Liu, and N. Zeng (2021). Ferulic Acid: A Review of Its Pharmacology, Pharmacokinetics and Derivatives. *Life Sciences*, **284**; 119921

Liu, H., H. C. S. Chan, X. Yu, J. Li, J. Li, and Z. Zhou (2023). Two Polymorphic Cocrystals of Theophylline with Ferulic Acid. *Crystal Growth & Design*, **23**(6); 4448–4459

Liu, L., J.-R. Wang, and X. Mei (2022). Enhancing the Stability of Active Pharmaceutical Ingredients by the Cocrystal Strategy. *CrystEngComm*, **24**(11); 2002–2022

Lu, T. (2024). A Comprehensive Electron Wavefunction Analysis Toolbox for Chemists, Multiwfn. *The Journal of Chemical Physics*, **161**(8)

Martín Pendás, A., E. Francisco, D. Suárez, A. Costales, N. Díaz, J. Munárriz, T. Rocha-Rinza, and J. M. Guevara-Vela (2023). Atoms in Molecules in Real Space: A Fertile Field for Chemical Bonding. *Physical Chemistry Chemical Physics*, **25**(15); 10231–10262

Miar, M., A. Shiroudi, K. Pourshamsian, A. R. Oliaey, and F. Hatamjafari (2020). Theoretical Investigations on the HOMO–LUMO Gap and Global Reactivity Descriptor Studies, Natural Bond Orbital, and Nucleus-Independent Chemical Shifts Analyses of 3-Phenylbenzo[d]thiazole-2(3H)-imine and Its Para-Substituted Derivatives: Solvent and Substituent Effects. *Journal of Chemical Research*, **45**(1–2);

147–158
Neopane, D., V. A. Ansari, and A. Singh (2023). Ferulic Acid: Signaling Pathways in Aging. *Drug Research*, **73**(06); 318–324
Nyamba, I., C. B. Sombié, M. Yabré, H. Zimé-Diawara, J. Yaméogo, S. Ouédraogo, A. Lechanteur, R. Semdé, and B. Evrard (2024). Pharmaceutical Approaches for Enhancing Solubility and Oral Bioavailability of Poorly Soluble Drugs. *European Journal of Pharmaceutics and Biopharmaceutics*, **204**; 114513
Paneru, T. R., M. K. Chaudhary, B. D. Joshi, and P. Tandon (2024). Cocrystal Screening of Benznidazole Based on Electronic Transition, Molecular Reactivity, Hydrogen Bonding, and Stability. *Journal of Molecular Modeling*, **30**(11); 378
Panzade, P., A. Wagh, P. Harale, and S. Bhilwade (2024). Pharmaceutical Cocrystals: A Rising Star in Drug Delivery Applications. *Journal of Drug Targeting*, **32**(2); 115–127
Pujiono, F. E., D. Setyawan, and J. Ekowati (2024). Hydrogen Bond Analysis of the p-Coumaric Acid-Nicotinamide Cocrystal Using the DFT and AIM Method. *Pharmacy Education*, **24**(3); 57–62
Pyrzynska, K. (2024). Ferulic Acid—A Brief Review of Its Extraction, Bioavailability and Biological Activity. *Separations*, **11**(7); 204
Singh, J. S., M. S. Khan, and S. Uddin (2023). A DFT Study of Vibrational Spectra of 5-Chlorouracil with Molecular Structure, HOMO–LUMO, MEPs/ESPs and Thermodynamic Properties. *Polymer Bulletin*, **80**(3); 3055–3083
Song, X., C. Liu, Y. Zhang, X. Xiao, G. Han, K. Sun, S. Liu, Z. Zhang, C. Dong, Y. Zheng, X. Chen, T. Xu, Y. Liu, and Y. Li (2023). Sustainable Extraction of Ligustilide and Ferulic Acid from AngelicaeSinensisRadix, for Antioxidant and Anti-inflammatory Activities. *Ultrasonics Sonochemistry*, **94**; 106344
Sulistyowaty, M. I., D. Setyawan, P. P. M. Prameswari, R. J. K. Susilo, T. Amrillah, E. Zaini, and S. A. H. Zidan (2024). A Comparison Study between Green Synthesis of Microwave Irradiation and Solvent Evaporation Methods in the Formation of p-Methoxycinnamic Acid-Succinic Acid Cocrystals. *Science and Technology Indonesia*, **9**(3); 629–636
Szewczuk, N. A., P. R. Duchowicz, A. B. Pomilio, and R. M. Lobayan (2023). Resonance Structure Contributions, Flexibility, and Frontier Molecular Orbitals (HOMO–LUMO) of Pelargonidin, Cyanidin, and Delphinidin Throughout the Conformational Space: Application to Antioxidant and Antimutagenic Activities. *Journal of Molecular Modeling*, **29**(1); 2
Tatsumi, Y., Y. Shimoyama, and S. G. Kazarian (2024). Analysis of the Dissolution Behavior of Theophylline and Its Cocrystal Using ATR-FTIR Spectroscopic Imaging. *Molecular Pharmaceutics*, **21**; 3233–3239
Thayyil, A. R., T. Juturu, S. Nayak, and S. Kamath (2020). Pharmaceutical Co-Crystallization: Regulatory Aspects, Design, Characterization, and Applications. *Advanced Pharmaceutical Bulletin*, **10**(2); 203
Tupe, S. A., S. P. Khandagale, and A. B. Jadhav (2023). Pharmaceutical Cocrystals: An Emerging Approach to Modulate Physicochemical Properties of Active Pharmaceutical Ingredients. *Journal of Drug Delivery and Therapeutics*, **13**(4); 101–112
Velmurugan, V., R. Nandini Asha, B. Ravindran Durai Nayagam, S. Kumaresan, and N. Bhuvanesh (2021). Synthesis, Characterization and Biological Activity of (Phenylthio) Acetic Acid:Theophylline Cocrystal. *Journal of Chemical Crystallography*, **51**(2); 225–234
Vilas-Boas, S. M., R. S. Alves, P. Brandao, L. M. A. Campos, J. A. P. Coutinho, S. P. Pinho, and O. Ferreira (2020). Solid-Liquid Phase Equilibrium of Trans-Cinnamic Acid, p-Coumaric Acid and Ferulic Acid in Water and Organic Solvents: Experimental and Modelling Studies. *Fluid Phase Equilibria*, **521**; 112747
Wang, N., J. Wang, X. Huang, T. Wang, X. Li, J. Yang, Y. Bao, Q. Yin, and H. Hao (2021a). A Selective Cocrystallization Separation Method Based on Non-Covalent Interactions and Its Application. *CrystEngComm*, **23**(7); 1550–1554
Wang, X., S. Zhang, H. Zhao, Q. Wang, Y. Zhang, H. Xu, X. Xia, and S. Han (2021b). Spectroscopic Investigation into the Binding of Ferulic Acid with Sodium Deoxycholate: Hydrophobic Force Versus Hydrogen Bonding. *Langmuir*, **37**(4); 1420–1428
Wong, S. N., M. Fu, S. Li, W. T. C. Kwok, S. Chow, K.-H. Low, and S. F. Chow (2024). Discovery of New Cocrystals Beyond Serendipity: Lessons Learned from Successes and Failures. *CrystEngComm*
Xia, M., Y. Jiang, Y. Cheng, W. Dai, X. Rong, B. Zhu, and X. Mei (2023). Rucaparib Cocrystal: Improved Solubility and Bioavailability Over Camsylate. *International Journal of Pharmaceutics*, **631**; 122461
Yadav, A., R. Chaudhary, A. S. Bahota, P. Prajapati, J. Pandey, A. Narayan, M. A. S. Al-Hanafi, P. Tandon, and V. R. Vangala (2024). Combined Spectroscopic and Quantum Chemical Study to Explore the Effect of Hydrogen Bonding in Hydrochlorothiazide-Nicotinamide Cocrystal. *Journal of Molecular Structure*, **1300**; 137208
Yu, Y. M., Y. Y. Niu, L. Y. Wang, Y. T. Li, Z. Y. Wu, and C. W. Yan (2021). Supramolecular Self-Assembly and Perfected *in vitro / in vivo* Property of 5 -Fluorouracil and Ferulic Acid on the Strength of Double Optimized Strategy: The First 5 -Fluorouracil-Phenolic Acid Nutraceutical Cocrystal with Synergistic Antitumor Efficacy. *The Analyst*, **146**(8); 2506–2519

